Integrated Biomaterials: Materials in Medicine (Peer-Reviewed Book)

Edited by Murugan Ramalingam, Ashutosh Tiwari,

Seeram Ramakrishna, and Hisatoshi Kobayashi

Copyright © 2011 VBRI Press, www.vbripress.com

ISBN: 978-81-920068-02, eISBN: 978-81-920068-18, DOI: 10.5185/ib-2011-01

1

1D~3D Nano-engineered biomaterials for biomedical applications

Hui Chen, Xiaokang Li and Yanan Du *

Department of Biomedical Engineering, School of Medicine,

Tsinghua University, Beijing 100084, China

Abstract

The pursuit for optimized performances in biomedical applications has led to the development of bioactive and biocompatible materials with well-defined structural and therapeutic features. Meanwhile, due to the unique biophysical & biochemical properties achieved in molecular-scale resolution, nano-engineered biomaterials have been gaining increasing attention with potential applications in tissue engineering, bio-imaging, drug delivery etc. In this chapter, we review diverse approaches employed in preparing a number of commonly-used nano-engineered biomaterials and their biomedical applications. We categorize the reviewed biomaterials into: 3D (i.e. nano-particle), 2D (i.e. nano-fiber), and 1D (i.e. nano-sheet), according to the number of dimensions in nano-scale; and illustrate the material selection, fabrication methods and applications respectively in each section.

Correspondence/Reprint request: Prof. Yanan Du, Department of Biomedical Engineering, School of Medicine,

Tsinghua University, Beijing 100084, China

E-mail: duyanan@tsinghua.edu.cn

Introduction

The last few decades witness the prosperity of material science which plays a crucial role in current biomedical science and technology development. The functions and applications of certain material are highly dependent on its physical and chemical properties. In particular, the unique properties exhibited by materials with defined nanoscale structures (similar length scale of biomolecules [1]) are increasingly being realized by researchers in biomedical field(2-5). As an example, the nanostructures of extracellular matrix (ECM) have been shown to govern the migration, differentiation, and fate of cells(6), which are critical for cell and tissue engineering applications. To nano-engineer biomaterials with desired properties and functions, it is of great importance to optimize the fabrication methodologies, apply tailored modification, and develop precise characterization methods.

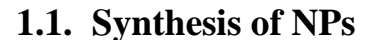
In this chapter, we reviewed recent progress on researches in nanoengineered materials, and their applications in biomedical fields such as tissue engineering, drug delivery, wound healing and medical implant. We define materials with all three dimensions in nano-scale as 3D nanomaterials such as nanoparticles, self-assembled peptide or DNA nanostructures(7); materials with 2 dimensions in nanoscale while the other dimension in micro/macro scale as 2-dimensional (2D) nanomaterials, such as nanofibers; materials with only one dimension in nanoscale while the other two in micro/macro scales as 1D nanomaterials such as nanosheets and nanofilters. All the nanomaterials in these three categories distinguish from their macro counterparts in many aspects such as optical(8), biocompatible(3), and elastic(9) properties. Due to the rapid development in nanomaterials, it is beyond the capacity of this chapter to provide an exclusive review. We therefore have mainly introduced one representative nanomaterials for each

category, namely nanoparticles for 3D nanomaterials; nanofibers for 2D nanomaterials; and nanosheets for 3D nanomaterials.

1. 3D nanomaterials towards biomedical applications

The most widely-used 3D nanomaterials are Nanoparticles (hereinafter referred to as NPs), which can be engineered into various shapes such as spherical, cubic, hollow or core shell. NPs have been attracting considerable interests due to their unique physical and chemical properties including desired optical and magnetic properties, specific heat melting points, and surface reactivities(1). These size-dependent properties of NPs are widely believed to be resulted from their high 'surface to volume ratio'.

NPs for biomedical applications can be synthesized from a variety of materials including inorganic materials and organic materials. Currently, the most well-developed NPs are synthesized from inorganic materials including noble metals (e.g. Au (10), Ag(11), Pt(12), Pd(13)), semiconductors (e.g. CdSe, CdS, ZnS(2,10), TiO2(14) (S(15), InP(15), Si(16)), magnetic compounds (e.g. Fe₃O₄(17), Co(18), CoFe₂O₄(19), FePt(13), CoPt(20)), and their combinations (core-shell NPs and other composite nanostructures). Compared to their natural counterparts, these inorganic NPs are usually easier and economical to synthesize and more stable. Organic NPs are commonly made from synthetic polymer (i.e. PLLA or PLA)(21,22) or natural biomolecules (i.e. DNA, RNA, proteins, or polysaccharide). These materials often have good biocompatibilities and are biodegradable(16). In the following parts, we review the methodology of synthesis, modifications, properties, and applications of 3D nanomaterials in biomedical fields.



NPs have been synthesized by both 'top down' and 'bottom up'



methods(23). 'Top down' method usually includes an initial step to grind the bulk materials into nano-scale particles followed by a stabilization step to prevent the NPs from aggregation. 'Bottom up' method is usually achieved by self-assembly of molecules in wet chemical reactions (for metallic NPs, reduction reaction is required)(23). A stabilization step is also essential. Since most NPs for biomedical applications are required to be stable and functional in aquatic environment, 'bottom up' method is more efficient and widely applied. A schematic is illustrated to describe the general process for NPs development for biomedical applications (Fig.1 section 1).

1.1.1. Synthesis in water

NPs with various compositions have been synthesized in aqueous solution such as Au(24,25), Ag(11), Co(26), Nix(27), Fe₃O₄, Fe₂O₃, FeO(OH)(28), SiO₂(29) and CdTe(30,31). Gold NPs can be prepared by reduction of Au (III) salts using reducing agents such as citric acid, sodium citrate, sodium ascorbate or amines(32). Iron (hydr)oxide NPs are synthesized by the alkali co-precipitation process, with the composition and morphology of the resultant NPs depending on the precise reaction conditions(28,33). Alkali precipitation is also suited for the preparation of more complex multi-metallic ferrites (34). Ag NPs can be synthesized following a green synthesis protocol where starch was used as a stabilizer(11). Synthesis of SiO₂ is well established via the Stober method(29). To develop environmentally benign technologies in NPs syntheses, Sastry and co-workers examined the possibility of using microbes and plant materials as nano-factories(35).

All the above-mentioned methods provide water-dispersible NPs, a necessity for the application in biological systems; however, control over particle size distribution is still limited. Since NP size tremendously affects their properties, a narrow size distribution is essential for controlled and reproducible performances(36). The nonuniformity of NPs can be reduced by

being treated with an apolar solvent containing hydrophobic ligand such as oleic acid, from which particles of the desired size may be obtained by size-selective precipitation(37).

1.1.2. Synthesis in organic medium

Synthesis in organic solvents have been published for a wide range of NPs composed of noble metals, transition metals, oxides and semiconducting materials(26,38-41). Growth, crystal structure and growth cessation depend on the composition of the organic medium and are fundamentally regulated by the addictives. Commonly-used organic medium for NPs synthesis are usually amphiphilic such as 4-dimethyl-aminopyridine (DMAP) (42). Addictives in the organic medium tend to be either surfactant species such as fatty acids or alkane thiols, rendering the particles highly hydrophobic which prevent the self-aggregation.

1.1.3. Other methods

Other methods for NPs synthesis have been reported including gel templating and solvent-free methods such as chemical vapor deposition (CVD) (43), electrical explosion (44) and mechanical milling (45). In gel templating, metallic NPs were crystalized in a nanoporous gel matrix after reductive reactions. Despite the wide applications of CVD, Electrical explosion and mechanical milling in producing NPs for heterogeneous catalysis, magnetic data storage and nanoelectronic devices, few successes have been achieved to apply NPs made by these methods in biomedical fields.

1.2. Structural and functional modification

In most cases, NPs have to be further modified to improve their biocompatibility or selectivity to achieve desired performances in biomedical applications. The modifications can be summarized as: 1) surface modification to functionalize or stabilize NPs; 2) internal modification to create hollow NPs with specific morphology or topology; 3) combination of the two above methods.

1.2.1. Surface modification

Surface modification (coating) can highly improve surface properties of NPs by introducing functional ligands and groups. In some cases, only the 'coatings' were left in the final products, whereas the core particles were dissolved. We reviewed the coating method for NPs according to the driving forces, namely: 1) by electrostatic forces, 2) by Van der Walls forces, 3) by covalent bonds.

1.2.1.1. Electrostatic force

Since 1991, layer-by-layer (LbL) assembly has been widely used as a modification method to improve surface properties of materials (46). As an example of LbL assembly mediated by electrostatic interactions, a charged substrate was first immersed into a solution containing an oppositely charged polymer [i.e. poly(allylamine hydrochloride) (PAH)](47). When the adsorption of the positively charged polymer reached equilibrium, the substrate was rinsed and immersed into a negatively charged polyelectrolyte solution [i.e poly(sodium 4-styrenesulphonate) (PSS)](47). The film thickness can be controlled by altering the number of layers deposited during the LbL assembly. When the desired thickness was obtained, the coated particles can be directly used in the core–shell state, or the core can be dissolved later to generate hollow polymeric capsules (Fig. 1, section 2).

1.2.1.2. Van der Walls force

When Van der Walls force is used as the driving force for coating NPs, core particles usually act as seeds during the modification process in which

monomers of the coating grow on the surface of these seeds. Here we present

two examples using Van der Walls force to coat a single layer or a porous meshwork on the core NPs. In the first case, Hua Xiao et al. reported a modification method to coat the surface of TiO2 NPs with Fe3O4 layer which was driven by Van der Walls force(48). In contrast to the un-modified TiO2 NPs, Fe^{3O4}:TiO² core-shell NPs generated red shift with higher absorption in visible region which led to improved efficiency to kill tumor cells by thermal-therapy and higher selectivity with minimum effects on normal tissues. In the second case, mesoporous SiO2 was grown on the surface of magnetic NPs, such as Fe3O4 nanocrystals cores, after the deposition of a thin layer of templating agent amorphous SiO2. The presence of a cetyltrimethylammonium bromide (CTAB) leads to the formation of mesoporous coating in the thickness of 2-4nm (Fig.1, section 3). The mesoporous SiO₂ coating allows loading of drugs, e.g. doxorubicin, ibuprofen, and other molecular species (49,50). Not only can the mesopores be used to deliver drugs, but they can also be used to scavenge biological species such as microcystins(51).

1.2.1.3. Covalent bond

Many functional biomolecules such as DNA, proteins, peptides and carbohydrates (Fig. 1, section 4) have been modified to the surface of NPs via covalent bond. As one of the strongest chemical interactions, covalent bonds enable stable linkage between functional molecules and NPs. For instance, extensive studies have been conducted to functionalize gold NPs via Gold-Sulfur-bond (Au-S bond). The modified functional molecules can offer additional properties to NPs including targeting, fluorescence and improved solubility etc(1). For example, Li et al. modified the AuNPs with a novel trithiol DNA oligonucleotide which had been shown to stabilize the Au NPs and increase their solubility in aqueous solution(52).



1.2.2. Internal modification

extends into the near-infrared region.

Internal modification is typically adopted to form porous hollow structures in NPs (PHNPs)(4). Compared with solid NPs with same sizes, PHNPs provide larger surface areas to encapsulate small molecules (53). Once loaded inside the porous structures, drug molecules are shielded by the shell from degradation and deterioration in physiological environment. The success of internal modification usually requires incorporation of sacrificing materials in NPs, which will be removed to generate the porous hollow structures. Next, we will provide two examples to show the details of the internal modification process. The first example of internal modification is achieved based on a template-assistance-annealing approach(54), in which the spindle-shaped akagenite (-FeOOH) NPs were first made and then coated with a thin layer of silica. The silica-coated spindle was subject to a thermal treatment at 500oC in air to convert the inner FeOOH core to porous hollow nanocapsule composed of haematite (-Fe2O3). The haematite nanocapsules with porous shells were recovered after the selective removal of the silica shell under a strong basic solution (Fig.1, section 5). The second example involves a procedure called galvanic replacement, in which the monodisperse Ag nanocubes were used as the sacrificial template for the formation of Au nanocages (Fig. 1, section 6) (55,56). Porous nanocages composed of Au/Ag alloy were successfully

synthesized which exhibit a tunable surface plasmon resonance peak that



1.3. Properties of nanoparticles for biomedical application

1.3.1. Toxity

Many materials that are supposed to be bio-friendly in bulk may become toxic when they exist as NPs. The molecular mechanism of NPs toxicity is mainly attributed to the induction of oxidative stress by free radical formation which could cause damage to biological components through oxidation of lipids, proteins, and DNA. The size, shape, surface chemistry of the NPs as well as degree of aggregation are all related to the production of free radicals and subsequent oxidative stress(57). The reticuloendothelial systems (RES) in organs such as the liver and spleen, are especially vulnerable to NPs, as they show slow clearance and tissue accumulation (storage) of the NPs. Additionally, organs of high blood flow, such as the kidneys and lungs, can also be affected when exposed to NPs (58). When introduced or absorbed into the systemic circulation, the interaction between NPs and blood components can lead to hemolysis and thrombosis. Besides, nanomaterial interactions with the immune system have been known to increase immunotoxicity as reviewed by Dobrovolskaia and McNeil (59). Currently, most studies have focused on acute toxicity, while investigations of long-term toxicity of the NPs are in demand for understanding the mechanism of nanotoxicology and wide application of NPs.

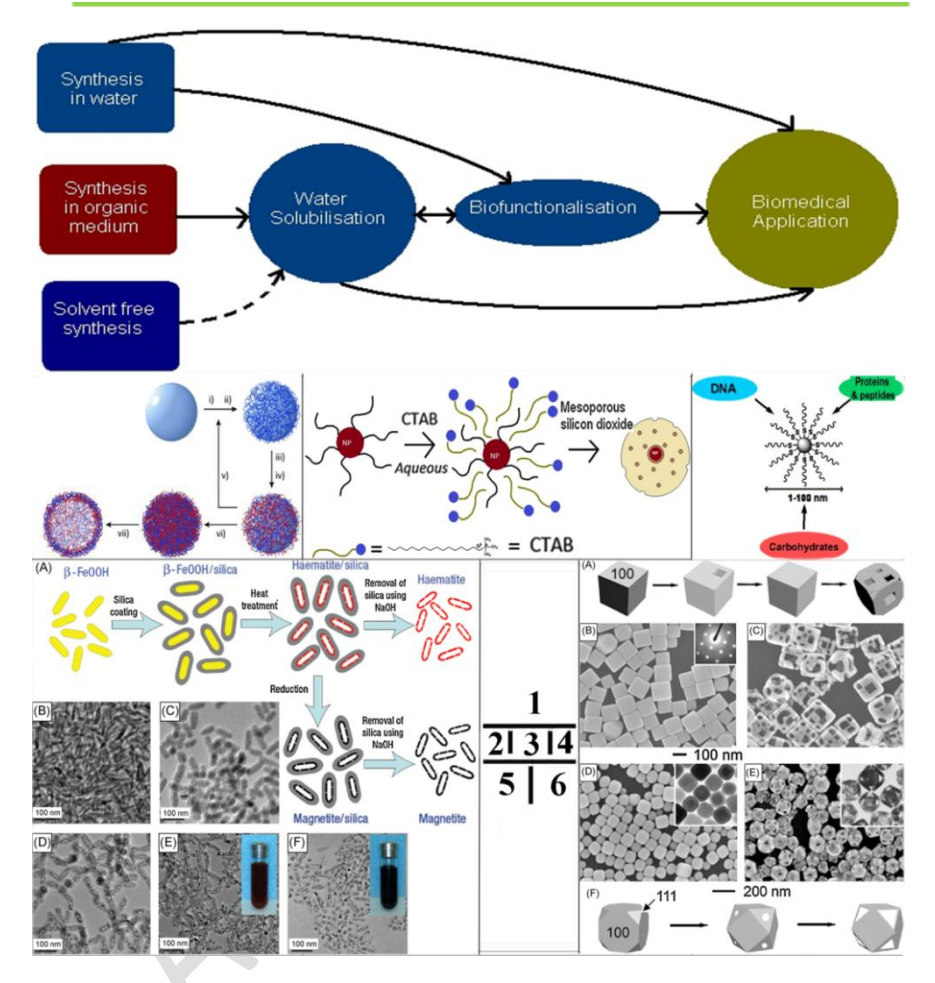


Figure 1. Fabrication and further modifications of nanoparticles

Section 1: Synthetic pathways of nanoparticles for biomedical application, the dotted line indicates that materials synthesized in solid state are not water soluble or may have no biomedical application. (Reprinted with permission from (60))

Section 2 : LbL assembly on NPs: i) Immersion in a positively charged polyelectrolyte solution; ii) rinse; iii) immersion in a negatively charged

polyelectrolyte solution; iv) rinse; v) repeat steps i—iv until desired number of layers has been deposited; vi) core—shell particles can be the end of the process, or vii) the template is dissolved off to leave a hollow polyelectrolyte capsule. (Reprinted with permission from (46))

Section 3: Use of CTAB in the conversion of hydrophobic NPs into mesoporous 'cargo transfer agents'. (Reprinted with permission from (60))

Section 4: Carbohydrates, DNA, proteins and peptides as biological coating for inorganic nanoparticles. (Reprinted with permission from (1))

Section 5: (A) Schematic illustration of the wrap-bake-peel process for the synthesis of iron oxide nanocapsules. (B~F)TEM images of FeOOH nanoparticles B); silica-coated FeOOH nanoparticles C); silica-coated iron oxide nanocapsules after the thermal treatment D); iron oxide nanocapsules after removal of silica shell E); reduced iron oxide nanocapsules after removal of silica shell F). (Reprinted with permission from (4))

Section 6: (A) Schematic illustration of morphological changes of an Ag nanocube into a Au/Ag nanobox then a predominately Au nanocage. SEM images showing the morphologies of (B) Ag nanocubes with sharp corners; (C) Au-based porous nanocages; SEM and TEM (inset) of (D) Ag nanocubes with rounded corners; (E) Au-based porous nanocages; (F) Schematic illustration of morphological changes. (Reprinted with permission from (4))

1.3.2. Optical properties

In general, as the sizes of semiconductor, metal and organic materials shrinks to nanoscale, their optical and electronic properties become size- and shape-dependent and largely vary from those in the bulk. The size- and shape-dependent properties at the nanoscale are attributed to the quantum confinement effect, i.e. strong confinement of electrons when the radius of a particle is below the excitation Bohr radius of the material. In a classical example, ancient Romans took advantage of surface plasmon resonance of the

Au NPs, which gives rise to brilliant red color to dye the glass. Among all the NPs which possess special optical properties, Quantum Dots (QDs) and noble metallic NPs are especially attractive for applications in optical devices, bioanalyses, and bioimaging because of their size-tunable luminescence(61) and plasmon color(62).

QDs are nano-scale semiconductor crystals composed of groups II-VI or III-V elements, and are defined as particles with physical dimensions smaller than the excitation Bohr radius. Semiconductor nanoparticles in the size ranging from 2nm to 6nm are of considerable interest due to their dimensional similarities with biological macromolecules (e.g. nucleic acids and proteins)(63). The distinctive optical property of QDs is represented by the size-dependent photoluminescence (PL) colors which are distributed throughout the visible region of the electromagnetic spectrum(61). The relation between the size and electronic band gap in semiconductor nanocrystals was developed by Luis Brus (64,65). According to the model, the semiconductor material used to synthesize QDs defines its intrinsic energy signature, while the size of QDs can determine the emission color. The size effect is especially significant near the band gap.

Like QDs, noble metallic NPs exhibit strong size-dependent optical resonance that is generally known as surface plasmon resonance (SPR). Under photo-activation, the plasmon couples with the excitation light and produces huge enhancement of the electromagnetic (EM) field in noble metal NPs(65). Interactions between the incident light and the oscillating electric fields result in the scattering and absorption of light. The SPR frequency depends not only on the metal, but also on the size and shape of the nanoparticle(62), the dielectric properties of the surrounding medium(66), and inter-nanoparticle coupling interactions. For gold (Au), silver (Ag), and copper (Cu), the resonance condition is fulfilled at visible frequencies (67), making them ideal choice for optical applications.

1.4. Applications of NPs

1.4.1. Biomedical Imaging

Due to excellent optical properties, gold NPs and ODs are among the most widely used NPs for biomedical imaging. Au NPs are well-known for its stability and inertness. Au NPs (10-50 nm in diameter) appear deep-red when in water or embedded in glass, a phenomenon that has fascinated people since ancient Roman times. The physical origin of this phenomenon is associated with the coherent oscillation of the surface electrons (localized surface plasmon) induced by the incident electromagnetic field (68). When visible light shines on Au NPs, the light of a resonant wavelength is absorbed by Au NPs and induces surface electron oscillation. For Au NPs with a diameter within a dozen nanometers, surface electrons are oscillated by the incoming light in a dipole mode. For instance, the solution will appear red when green light is absorbed (Fig.2 section 1B, red line). As the size increases, light can no longer polarize the nanoparticles homogeneously and higher order modes at lower energy dominate. This causes a red-shift and broadening of the surface plasmon band, which explains the color changes (red-to-purple) that are observed during the aggregation of small Au NPs (Fig.2 section 1B, blue line). When Au NPs aggregate, it could be considered as a single particle with larger size, although the detailed inter-particle plasmon coupling is rather complex and dependent on many factors, such as aggregate morphology and nanoparticle density. Au NP-based colorimetric biosensing assays have recently attracted considerable attentions in diagnostic applications(69) due to their simplicity and versatility (Fig.2 section 2). The key to the Au NP-based colorimetric sensing platform is the shift of colloidal Au NP dispersion and aggregation stages in the presence or absence of biological substances of interest (or analytes). The ability to balance inter-particle attractive and

repulsive forces is central in the design of such systems which determine whether Au NPs are dispersed or aggregated and consequently the color of the solution. Aggregation of Au NPs in these assays can be induced by an 'inter-particle-crosslinking' mechanism in which the enthalpic benefits of inter-particle bonding formation overcome inter-particle repulsive forces.

As another widely-used NPs in biomedical imaging, the favorable optical properties of QDs rely on confined excitations in all three spatial dimensions. When hit by a photon in the visible light region, electrons of QDs are excited to enter higher energy states, and then emit a photon with characteristic frequency when returning to the ground state. The narrow emission and broad absorption spectra of QDs makes them well-suited for multiplexed imaging (Fig.2 section 4), in which multiple colors and intensities are combined to encode genes, proteins and small-molecule libraries (70). Zhang et al. designed a DNA nanosensor based on Fluorescence Resonance Energy Transfer (FRET) from QD605 and a fluorescence dye Cy5 as a donor-acceptor pair(71). In the absence of targeted DNA, there was no FRET and the Cy5 could be excited by 488nm light. When a target DNA sequence was present, the Cy5 dyes were linked to the QDs mediated by base-pairing among the capture probe/target DNA/reporter probe (Fig.2 section 3). Therefore, when the nanosensor were excited by 488nm light, the Cy5 could be excited through FRET with the QDs. The selection of QD605 and Cy5 as a donor-acceptor pair allowed negligible crosstalk and selection of a wavelength near the minimum absorption spectrum of the Cy5.

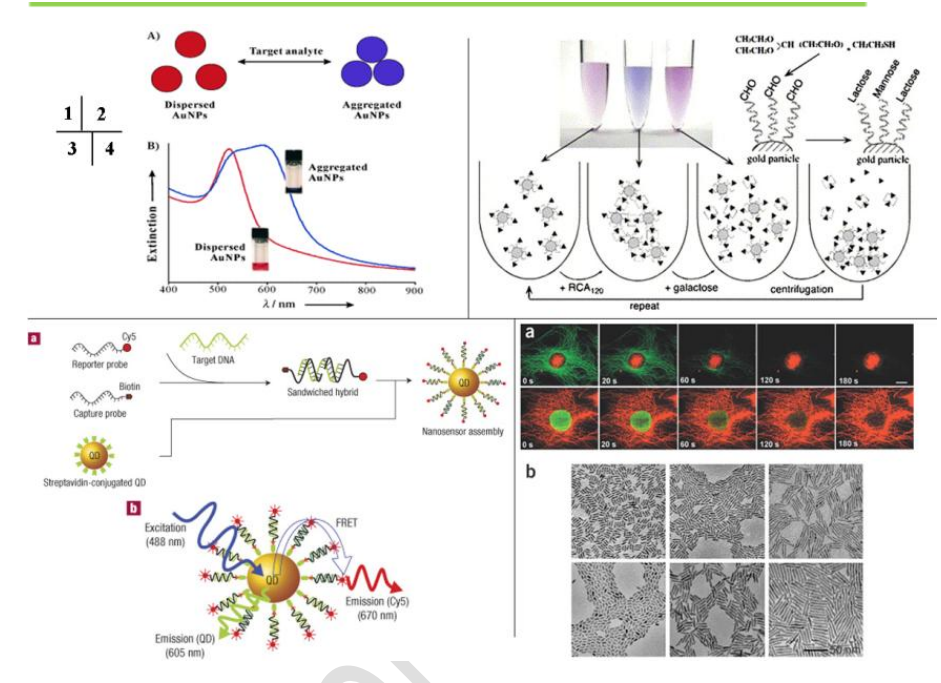


Figure 2. Nanoparticles employed in biomedical imaging

Section 1: A) Schematics illustrating absorption-based colorimetric Au NP biosensing assays by using Gold NPs aggregation and dispersion. B) Typical plots of surface plasmon absorption for 13 nm Gold NPs in the visible light region. Dispersed and aggregated Au NPs were represented by red and blue curves respectively. (Reprinted with permission from (8))

Section 2:Schematics illustrating the reversible aggregation-dispersion behavior of lactose gold NPs by sequential addition of RCA₁₂₀ lectin and galactose with immediate change in color from pinkish-red to purple to pinkish-red. Reprinted with permission from Reference citation 69 (Kataoka's group). Copyright 2001 American Chemical Society.

Section 3: Schematics of DNA nanosensors based on single-QD. (a) Conceptual scheme illustrating the formation of a nanosensor assembly in the presence of targets.

(b) Fluorescence emission from Cy5 on illumination on QD by FRET between Cy5 acceptors and a QD donor in a nanosensor assembly. (Reprinted with permsision from (71))

Section 4: Quantum confinement in new biological labels and semiconductors. (a) Cell labeling with quantum dots and representation of quantum dot photostability, compared with Alexa 488. In the top panels, the nucleus is stained red with quantum dots and the actin fibers are stained green with Alexa 488. In the bottom panel, the labeling is reversed. (b) Transmission electron micrographs of quantum rods that may be used as a biological label with polarized emission, reduced blinking and faster radiative rates than QDs. (Reprinted with permission from (72))

1.4.2. Analytical tools

Due to the large surface area, NPs can function as a carrier for recognition agents such as antibodies which can be used to concentrate the corresponding targets and amplify the detection outcome. Lin et al. reported the use of carbohydrate-encapsulated AuNP (c-AuNP) as an affinity probe for the efficient separation and enrichment of target proteins(73) (Fig. 3 section 1). A lectin (PA-IL) was successfully isolated from a mixture of proteins and detected at femtomole concentrations using glucose nanoparticles and MS (mass spectrometry) analysis. The methodology allows enrichment of the targeted peptide and following identification of its binding sequences to the carbohydrate.

1.4.3. Therapeutic biomedicine

NPs have been used as anti-adhesive layers to prevent adhesion of cancer cells to the target tissues. One of the critical steps in cancer metastasis is the adhesion of tumor cells to the vascular endothelium(1). Upon adhesion, tumor cells transmigrate and create new tumor foci. Tumor adhesion is mediated by

the carbonhydrate-carbonhydrate interactions between tumor-associated antigens and epithelial cell selectins. Therefore, blocking the binding sites in the tumor cells to the endothelium was proposed as a potential anti-adhesion therapy. J.M. de la Fuente et al. used glyconanoparticles that present carbohydrate antigens expressed either in the tumor or the endothelium cells to inhibit tumor cell adhesion (Fig. 3 section 2). An ex vivo experiment was designed for the evaluation of the anti-metastasis potential of the glycol nanoparticles. Mice were injected with melanoma cells pre-incubated with lactose gold glycol nanoparticles. After 3 weeks, a 70% of tumor inhibition was reported as compared with the group inoculated only with melanoma cells.



1.4.4. Drug delivery

Drug delivery systems provide an effective tool for enhancing the efficacy of pharmaceuticals through improved pharmacokinetics and biodistribution. The size of NPs allows them to cross cellular membranes and escape from the detection by the reticuloendothelial system. Their high surface to volume ratio can also allow increased loading of therapeutic agents. In particular, incorporation of magnetic or thermal sensitive components in the NPs can create remotely-controlled drug delivery systems. Wakamatsu et al. succeeded preparation of magnetic nanoparticles conjugated with a poly(N-isopropylacrylamide (PNIPAAm) temperature-responsive polymer(74). This nanoparticle system showed а sensitive and reversible hydrophilic-hydrophobic change in response to the heat induced by an field. oscillating magnetic These temperature-responsive nanoparticles contain carboxyl groups, which were used as the binding point of the drug (Fig. 3 section 3). By adjusting the intensity of magnetic heating, the profile of drug release could be regulated from gradual release to burst release.

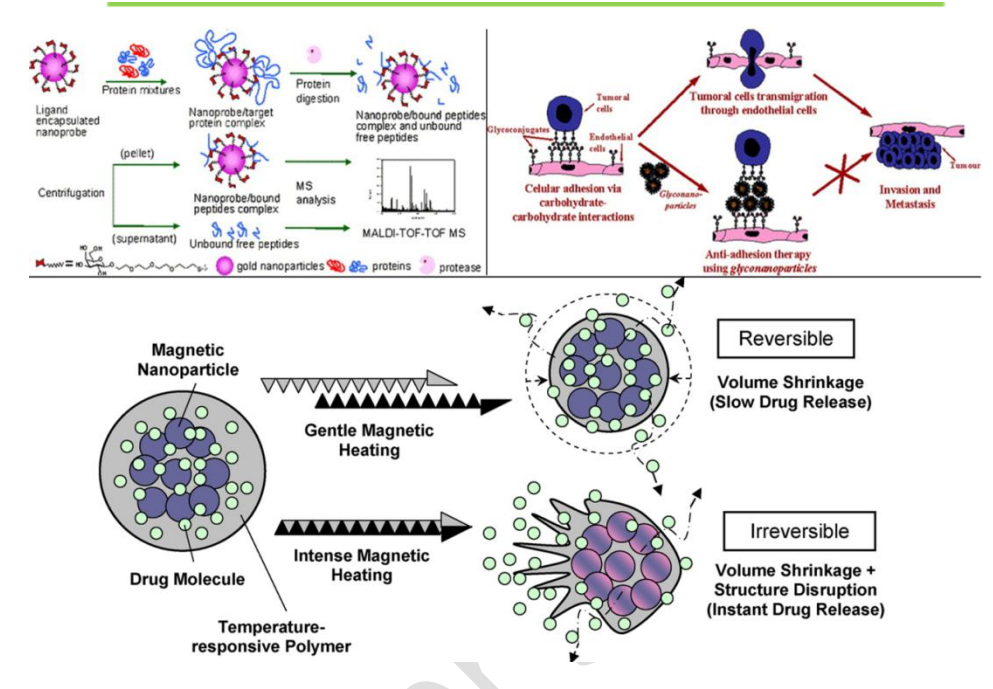


Figure 3. Other applications of NPs. (Section 1~3: top left, top right and bottom)

Section 1: Scheme of the specific capture of target proteins and the rapid mapping of binding-epitope-containing peptides. (Reprinted with permission from (1))

Section 2: Possible action mechanism of lactose glyconanoparticles in anti-adhesive therapy.(Reprinted with permission from (1))

Section 3: Two drug release mechanisms under magnetic heating. Gentle magnetic heating causes temperature-responsive polymer to shrink, squeezing drug out of NPs. Intense magnetic heating additionally ruptures the nanoparticle, triggering a burst-like drug release, causing irreversible release. (Reprinted with permission from (17))

2. 2D nanomaterials towards biomedical applications

2D nanomaterials are defined as materials with two dimensions in nanoscale, such as nanofibers, nanotubes, nanowires, and nanorodes. All the listed 2D nanomaterials above are the subjects of fundamental and technological interests because of their unique properties arising from high aspect ratios and large surface areas as well as their optical and electronic responses(75). We will review the development of nanofibers, which is one of most widely-used and well-developed 2D nanomaterials, mainly focusing on the raw materials' selections, fabrication strategies, and applications in biomedical fields.

2.1. Materials of nanofiber

Nanofibers with potential biomedical applications are usually synthesized from a wide variety of biocompatible materials that can be formed into nanofibrous structures. The materials of the Nanofibers determine the mechanical properties, degradation rates, and cell-material interactions. The commonly-used materials to synthesize nanofibers and nanowires are from naturally occurring extracellular matrix (ECM) which are ideal materials for cell adhesion, survival, proliferation, and differentiation. ECMs used for fabrication of nanofibers include collagen, gelatin, elastin, chitosan, dextran, fibringen, laminin, hyaluronic acid [75-77]. Compared to ECMs, synthetic polymers are usually easier to fabricate, more controllable and more stable showing better mechanical properties. However, surface modification is usually required to improve the bioactivity of the synthetic materials for biomedical engineering such as tissue engineering. Commonly-used synthetic polymers include poly(lactide-co-glycolide) (PLGA), 2,2'-bis-[4-(methacryloxypropoxy)- phenyl]- propane (bis-GMA), tri-ethylene glycol dimethacrylate (TEGDMA) and poly(acrylic acid)-poly(pyrene

methanol) (PAAPM)(76).

2.2. Fabrication strategies

A variety of techniques based on physical, chemical, thermal, or electrostatic principles, have been adopted to fabricate 2D nanomaterials for biomedical applications. The most used methods include electrospinning, self-assembling and phase separation(77,78). Examples of these fabrication methods (Fig. 3) are briefly summarized in table 1 which also includes the advantages and disadvantages of each method. (79)

2.3.Biomedical applications of 2D nanomaterials

Due to the structural mimicry with natural materials, nanofibers exhibit intrinsic advantages for biomedical and biotechnological applications. A great variety of natural biomaterials exist in fibrous forms or structures and are characterized by well-organized hierarchical fibrous structures down to nanometer scale(76), such as silk, keratin, collagen, viral spike proteins, tubulin, actin, polysaccharide cellulose and chitin. In the following part, an overview is given on the recent applications of nanofibers in tissue engineering, controlled drug delivery, dressings for wound healing and biosensors.

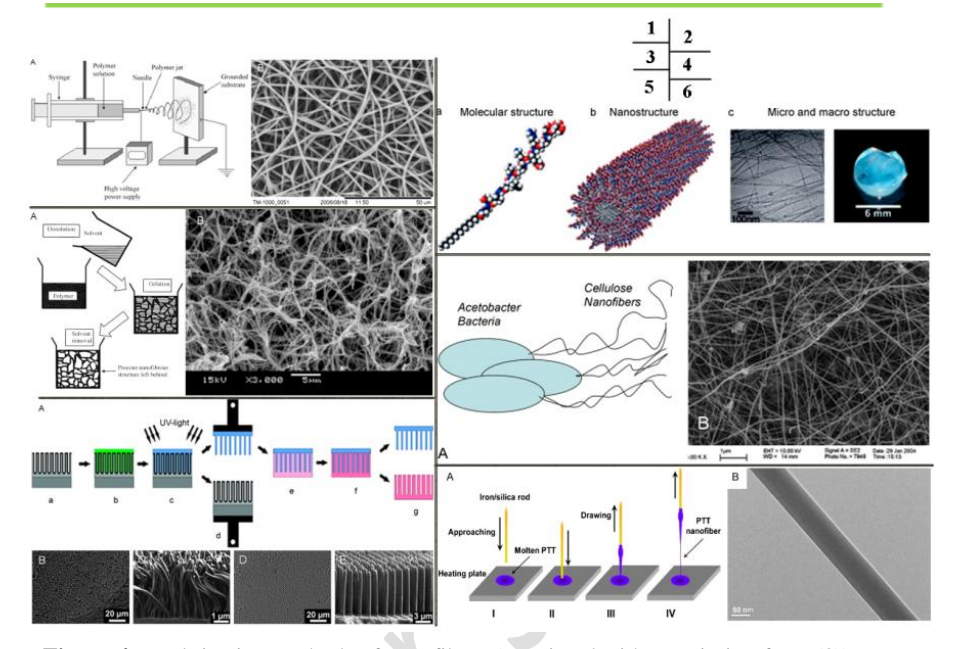


Figure 4. Fabrication methods of nanofibers (Reprinted with permission from (3))

Section 1: (A) Scheme of a standard electrospinning setup; (B) A scanning electron microscope (SEM) image of electrospun polyurethane nanofibers.

Section 2: (A) Scheme of the molecular structure and (B) nanostructure; (C) images of the micro and macro structure of a self-assembling peptide-amphiphile nanofiber network

Section 3: Schematic (A) of nanofiber formation by phase separation; (B) SEM image of nanofibrous structure fabricated by the above technique.

Section 4: (A) Schematic of Acetobacter cells depositing cellulose nanofibers; (B) SEM image of a cellulose nanofiber mesh produced by bacteria.

Section 5: (A) Schematic of the fabrication of polymer nanofibers using a nondestructive templating technique (grey: alumina template, green: resin, blue: polymer nanofibers, pink: silica replica template. (B) SEM images of 120 nm (B&C) and $1\mu m$ (D&E) polymer fibers fabricated by the above technique.

Section 6: (A) Schematic of the extruding technique to fabricate nanofiber. (B) Transmission electron microscope (TEM) image of a polymer nanofiber fabricated by the above technique.

 Table 1.

 Description and comparison of methods for fabricating polymeric nanofibers

Dimensions	Advantages	Disadvantages	Ref	Ξ		
Electrospinning (Fig. 4 Section 1)						
A 'top-down' approach. The simplest setup consists of only a syringe or pipette to hold						
an electrically charg	an electrically charged polymer solution, two electrodes and a DC high voltage power					
generator to extrude	generator to extrude the polymer solution into nanofibers.					
Diameter: 3 nm	•Easy to setup	•Poor cell infiltration into	(80-82))		
to several	•Cost effective	the core of the scaffolds				
micrometers;	•High level of versatility	for tissue engineering				
Length:	allows control over fiber	•2-Dimensional pore or				
continuous	diameter, microstructure	microstructure				
	and arrangement	arrangement				
	•Vast materials selection	•Toxic solvents often				
		used				
Self-Assembly (Fig. 4 Section 2)						
A 'bottom-up' approach. A process whereby atoms, molecules or macromolecules						
organize and arrange themselves through weak and non-covalent forces such as						
hydrogen bonding, electrostatic interactions, and hydrophobic forces into stable and						
structurally well-def	ined functional entities at the	nanoscale dimensions.				
Diameter: well	•Easy incorporation of	•Complex and costly	(82)			
below 100 nm;	cells during Fiber	procedure				
Length: up to few	formation	•Lack of control of fiber				
micrometers.	•3-Dimensional pore	orientation and				
	arrangement	arrangement				
	•Injectable for in vivo	•Limited fiber				

	assembly	diameter~2-30nm and				
		length~10 μ m				
Phase Separation (Fig. 4 Section 3)						
Typically co	nsisting of five steps, i.e	. raw material dissolution	n, phase			
separation/gelation,	solvent extraction and freeze-	drying.				
Diameter : 50 to	•3-Dimensional pore	•Complex procedures	(83,84)			
500 nm;	arrangement	•Lack of control of fiber				
Length: few		arrangement				
micrometers						
	Bacterial Cellulose (Fig	g. 4 Section 4)				
Utilize bacteri	ias to polymerize of glucose	residues into chains, followe	ed by the			
	on, assembly and crystallizat					
composed ribbons.	,		J			
Diameter: less	•Low cost	•Limited material	(85)			
than 100nm;	•High yield	selection	, í			
Length:	2 ,	•Lack of versatility for				
continuous		functionalization				
	Templated Growth (Fig	g. 4 Section 5)				
To use commo	ercially available nanoporous		unthesize			
or extrude nanoscale		memoranes as template to s	ynthesize			
		-Ca-miff sigl	(96)			
Diameter : a few	•Vast materials selection	•Sacrificial materials	(86)			
to hundreds nm;	•Control over fiber	•Limitation on fiber				
Length:	diameter and length	dimensions and				
micrometers		arrangement				
Extruding (Fig. 4 Section 6)						

Mechanically draw from viscous polymer liquids directly.					
Diameter: 60nm	•Vast materials selection	•Low productivity(One	(87)		
to 500nm	•Simple procedure	single fiber at a time)			
Length:		•Difficult to form fibers			
continuous		with consistent diameter			

2.3.1. Tissue Engineering

Natural ECM fibers such as elastin, collagen and keratin play a crucial role in tissue and organ development and regeneration by providing both biological and physical support for cell attachment, proliferation, migration, differentiation and ultimately cell fate(88). Meanwhile, synthetic nanofiber scaffolds have been shown as a promising substitute of natural ECM fibers for engineering tissues such as cartilages (89-92), bones(92), arterial blood vessels (93-95), heart (96), and nerves (97). Polymeric nanofiber scaffolds can be designed in a way that predictably modulates a variety of important cell behaviors directing favorable functions. The nano topography itself, independent of the fiber material and chemical signals, has demonstrated the possibilities to direct cell behaviors(88) desirable in tissue engineering such as unidirectional alignment; increased viability, attachment, and production; guided migration; and controlled differentiation. Because cells can react to objects as small as 5 nm, which are some 1,000-5,000 times smaller than the sizes of themselves (98,99)



2.3.2. Drug delivery

For controlled drug delivery, in addition to their large surface area to volume ratio, 2D nanomaterials also exhibit additional advantages. For example, unlike common encapsulation involving complicated preparation process, therapeutic compounds can be conveniently incorporated into the

carrier polymers and encapsulated in the resulting nanofibers upon electrospinning(100). The resulting nanofibrous membrane containing drugs have be applied topically for skin and wound healing, or post-processed for other kinds of drug release(100).

2.3.3. Wound healing

Nanofibers have been also used as dressing to promote hemostasis and wound healing [100]. An ideal dressing can provide an environment at the surface of the wound to accelerate healing with an acceptable cosmetic appearance (76). In this example, hemostasis was activated simply from the physical feature of the nanofibrous dressings but without using a haemostatic agent. Besides the direct activation effect, nanofiberous dressing can absorb wound exudates more efficiently than film dressing(76). In addition, Zong et.al. have implated poly(lactideco-glycolide) nanofibrous membrane between cecum and abdominal wall which effectively reduced the post-surgery-induced abdominal adhesions and could act as a physical barrier as well as a local drug delivery vehicle (101).

2.3.4. Biosensors

Biosensors for biomedical applications typically consist of biofunctional membrane for sensing and transducer for signal generation. Performances of a biosensor are highly dependent on the property of the sensing membrane. The high surface to volume ratio makes the nanofibrous membrane a favorable material of choice for sensing membranes, which are expected to significantly improve the sensitivity, selectivity, response time, reproducibility of the biosensor. Lowell et al. (102,103) demonstrated that biosensors made from electrospun nanofiber (100–400 nm in diameter) membranes containing fluorescent poly(acrylic acid)-poly(pyrene methanol) (PAAPM) for detecting metal ions (Fe³⁺ and Hg²⁺⁾ and 2,4-dinitrotulene (DNT) exhibited a sensitivity

of almost three orders of magnitude higher than that of thin films made from the same material.

3. 1D nanomaterial towards biomedical applications

In this section, we summarize recent studies related to nanomembrane, one of the most representative 1D nanomaterials. The most important and distinctive property of 1D nanomaterials is their extremely high aspect ratio (usually greater than 10⁶) which gives these materials a number of new traits. For instance, inorganic nanomembranes (i.e. silicon nanomembranes) show greater flexibility than their rigid bulk counterparts while maintaining good mechanical properties(104). Nanomembrane can be formed either on a solid support or in a free-standing status (called freestanding ultrathin nanomembranes, FUN-membranes). When formed on a solid support such as glass or silicon wafer, the nanomembrane usually cannot function alone, which significantly limit their potential applications (Fig. 5A, B). While the FUN membranes are stable and self-functional which show more potential for biomedical applications (Fig. 5C). Thus, our summary will be focused on the methodology of fabrication, characterization, and applications of the FUN-membranes

3.1. Fabrication strategies

Currently FUN-membranes have been mainly fabricated from 'top-down' and 'bottom-up' approaches. Top-down lithographic-based techniques have been widely used to directly generate nanostructures on the membrane (105-107). However, the 'top-down' approaches are usually time-consuming and require high-end facilities. Alternatively, 'bottom-up' approaches for FUN-membrane fabrication can potentially overcome these limitations replying on self-assembly process which is rapid and inexpensive. Moreover,

'bottom-up approach' is capable of efficiently fabricating organic-based nanomembranes (i.e. PNIPAAm) which, unlike their inorganic counterparts, can be used in soft and 'smart' devices that can operate dynamically in response to a variety of stimuli including light, pH, temperature and electric or magnetic fields(108).

Formation of the UN-membranes by 'bottom-up' self-assembly requires confinement in one-dimension to generate the nanoscale thickness. Typically, it can be achieved at a two-dimensional interface, such as a solid support or fluid-fluid interface or even within an empty hole (Fig. 5)

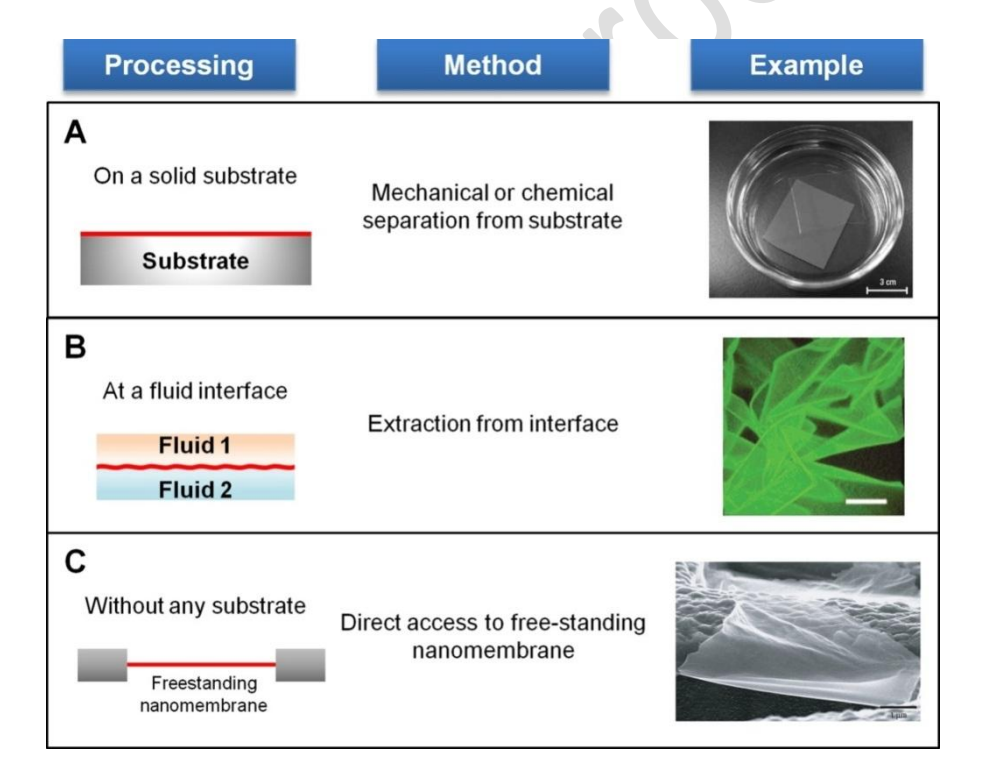


Figure 5. Fabrication of FUN-membranes. (A) Nano-membranes can be first assembled

on a solid substrate and subsequently separated from the substrate via either mechanical or chemical means. (B) Nano-membranes can also be extracted after assembly at a fluid interface. (C) Direct access to FUN-membranes can be achieved by assembly within a hole. (Reprinted with permission from reference (104))

3.1.1. Transfer from solid surfaces

Assembly on solid substrates is the most common approach to fabricate FUN-membranes which can be reliably achieved by applying techniques such as layer-by-layer (LbL) assembly, Langmuir – Blodgett (LB) transfer, spin-coating, electrophoretic deposition and crosslinking of self-assembled monolayers (SAMs). Each of the above techniques offers varying degrees of control over membrane thickness, composition and stability. However, harvest of the FUN-membrane typically requires removal or transfer of the membrane from the substrate, either by physical detachment or by chemical dissolution of a sacrificial layer. The conditions of the detachment process should be optimized since harsh conditions such as chemical dissolving of the sacrificial layer could potentially alter the surface properties of the nanomembrane and compromise its integrity.

3.1.2. Extract from fluid interfaces



The fluid interface serves as a mobile substrate for the membrane assembly. FUN membranes formed at the fluid-fluid interfaces can be readily extracted, thus avoiding the detachment step associated with the assemblies at solid substrates. The self-assembly on the liquid-liquid interface is mainly driven by the minimization of free energy, which is partially resulted from thermal fluctuations and interfacial energy (109-111).

Liquid-air interfaces are versatile platforms that have been widely used for assembling FUN-membranes. Y. Hong et al.(112) have reported that

polymerizable silicate precursors interact with a surfactant template assembled at the water-air interface, leading to the formation of a smooth and continuous mesoporous silica membrane. Notably, these nano-membranes are extremely resilient, yet sufficiently flexible for transferring onto a variety of substrates. In addition, hydrophobic polyisoprene monolayers can self-assemble at the water-air interface. Photocrosslinking the polyisoprene monolayers could further enhance the mechanical stability and facilitated the transfer of the resulting elastomeric membranes onto solid supports (113,114). Porous freestanding membranes were also obtained based this technique(115). Silica colloidal particles were first incorporated into the monolayers. which were subsequently crosslinked. polvisoprene The silica particles were then removed by exposure to hydrofluoric acid vapor, vielding porous freestanding structures.

3.1.3. Microhole-mediated assembly

Drying-mediated nanoparticle assembly on a solid substrate is notorious for its lack of control over the uniformity of nanoparticle films. This is because self-assembly drying-mediated on solid surface far-from-equilibrium effects such as fluid flows and solvent fluctuations during the late stages of the dewetting process, which leads to non-uniform nanoparticle deposits(116,117). Cheng et al. demonstrated that the limitations associated with these stochastic processes could be overcome by molding colloidal microdroplets. This affords rational control over the local nucleation and growth of nanoparticle super-lattices by spatially regulating the dewetting process(118). Furthermore, this spatial confinement of the drying-mediated process could be performed within microholes, which yielded freestanding membranes reaching the limit of their thickness(119).

3.2. Micromechanical Characterization

Micromechanical properties, such as the elastic modulus, ultimate strength and maximum elongation, are key parameters for evaluating the performances of FUN-membranes. Micromechanical analysis techniques typically involve the response of the material as a whole to externally applied forces, from which mechanical and rheological information can be extracted.

3.2.1. Bulging test

The bulging test(Fig. 6A) is one of the earliest techniques that has been used to characterize the mechanical properties of thin membranes(120), but has recently been applied to FUN-membranes (113,121,122). This technique involves the clamping of a membrane on a solid support, suspended over circular or square hole. An overpressure is applied to one side, causing the membrane to expand in the opposite direction (Fig. 6A). The relationship between the pressure difference, P, and the observed membrane deflection, d, is given by (120)

$$\Delta P = \left[C_0 \frac{E}{1 - v^2} \frac{h^4}{R^4} + C_1 \frac{\sigma_0 h^2}{R^2} \right] \left(\frac{d}{h} \right) + C_2 \frac{E}{1 - v} \frac{h^4}{R^4} \left(\frac{d}{h} \right)^3$$

Where E is the elastic modulus, h is the membrane thickness, R is the membrane radius, σ_0 is the pre-stress, and v is Poisson's ratio. C_0 , C_1 , and C_2 are coefficients that depend on the membrane geometry.

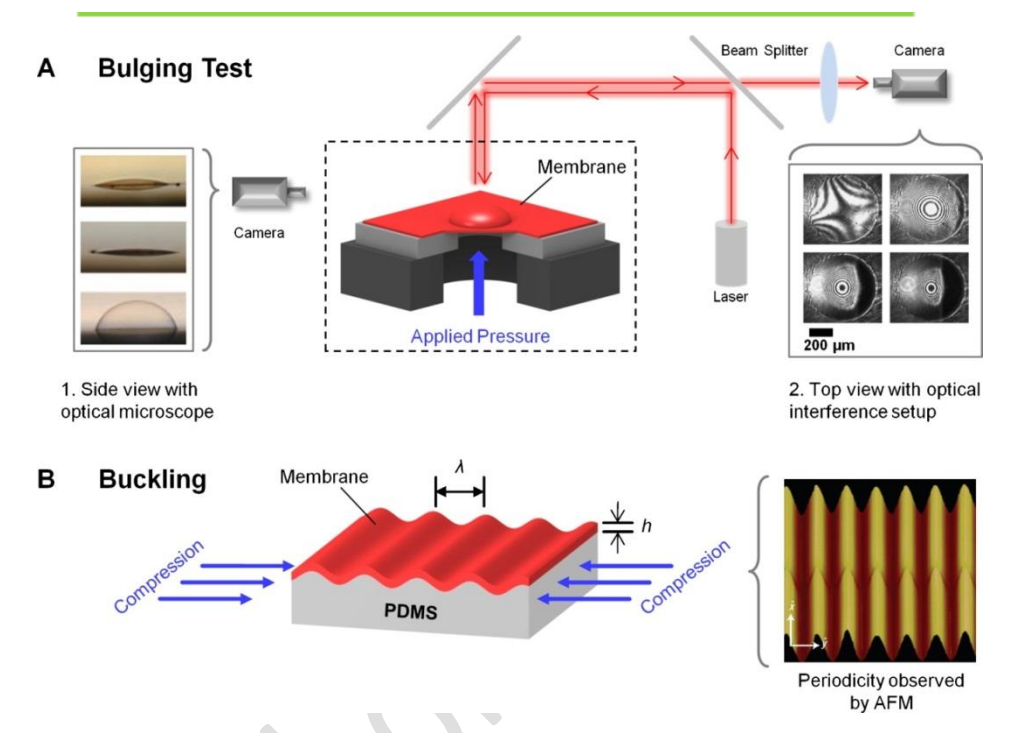


Figure 6. Micromechanical assessment of nanomembranes. (A) A bulging test measures the response of a suspended membrane to an overpressure. The membrane deflection is measured to produce a pressure vs. deflection curve, from which mechanical parameters can be extracted. The deflection can be measured optically either by viewing the film from the side (left) or by using an interferometry setup (right). The rings of the interference pattern can be correlated to the membrane deflection. (B) In a buckling test, the membrane is transferred to a PDMS substrate which is subjected to a compressive force. This produces a periodic buckling pattern in the membrane, which can be observed by AFM. The period, λ , of the buckling deformation can then be used to compute the elastic modulus. (Reprinted from reference (104))

3.2.2. SIEBIMM

Another emerging powerful method for measuring the elastic moduli of FUN-membranes is the 'strain-induced elastic buckling instability for mechanical measurements' (SIEBIMM) technique(123) (Fig.6B). Conventional mechanical testing devices typically lack of sensitivity to measure the forces involved in straining a thin polymer film. Nanoindentation has proved successful in mechanical testing of thin film such as ceramics and metals, but it is still challenging to test soft materials, especially those of exhibit sub-micrometre thickness, or those significant viscoelastic behaviors(124). C. M. Stafford et al. designed a new bulking based system named SIEBIMM (123), a technique that rapidly measures the elastic modulus of coatings and films. This technique exploits a buckling instability that occurs in bilayers consisting of a stiff, thin film coated onto a relatively soft, thick substrate. According to the spacing of these highly periodic wrinkles, they calculated the film's elastic modulus by applying the theory in well-established buckling mechanics. This new measurement platform has been applied for measurement of several FUN membranes playing a wide range of thicknesses (nanometre to micrometre) and moduli (MPa to GPa).

3.3. Applications toward biomedical field

FUN-membranes have been found useful in a wide variety of applications including as nano-separation membranes for purification, and as nanosensors for electrochemical and photochemical detection(108). With the emerging of biocompatible and biodegradable FUN-membranes, their great potential for biomedical applications has been increasingly exploited.

Yosuke Okamura and coworkers developed free-standing PLLA nanomembranes with thickness of 20nm(125). The nanomembranes were fabricated by a simple combination of spin-coating and peeling-off methods

with poly (vinyl alcohol) (PVA) as a supporting and sacrificial film (Fig. 7 Section i). The ultra-thin PLLA nanomembrane was found to have an excellent sealing efficacy for gastric incision as a novel wound dressing that does not require adhesive agents. Furthermore, the sealing operation repaired the incision completely without scars and tissue adhesion and it also shows great promise in reduction of operation times. Kevin Kit Parker et al. successfully engineered artificial FUN-membranes to mimic natural ECMs for cell culture and tissue engineering(126). To rebuild the ECM structure with multifunctional, nano to micrometer scale protein fibrils in vitro, the authors developed a surface-initiated assembly technique (Fig. 7 Section ii). The matrix proteins (i.e. fibronectin, laminin, fibrinogen, collagen type I, and collagen type IV) were micro-patterned onto thermo sensitive surfaces in 1 to 10nm thick, micrometer to centimeter wide networks, and released as flexible and free-standing nanofabrics.

4. Conclusion

With the maturation of nanotechnology as a rising discipline and its integration with biomaterial field, nanoengineered materials have been shown with great potential for biomedical plications. In this chapter, we provide an overview of biomedine-related manomaterials. Based on the number of dimensions in nano-scale, we categorize the reviewed commaterials into 3D, 2D and 1D. Within each category, we have focused on the most representative nanomaterials, namely nanoparticle, nanofiber and nanomembrane. We illustrated the material selection, fabrication methods, characterization and existing biomedical applications and discussed potential problems such as the cytotoxicity. It is expected that the emerging nanomaterials with well-controlled structural and functional properties will play an increasingly

vital role as powerful tools to fulfill the needs in biomedicine.

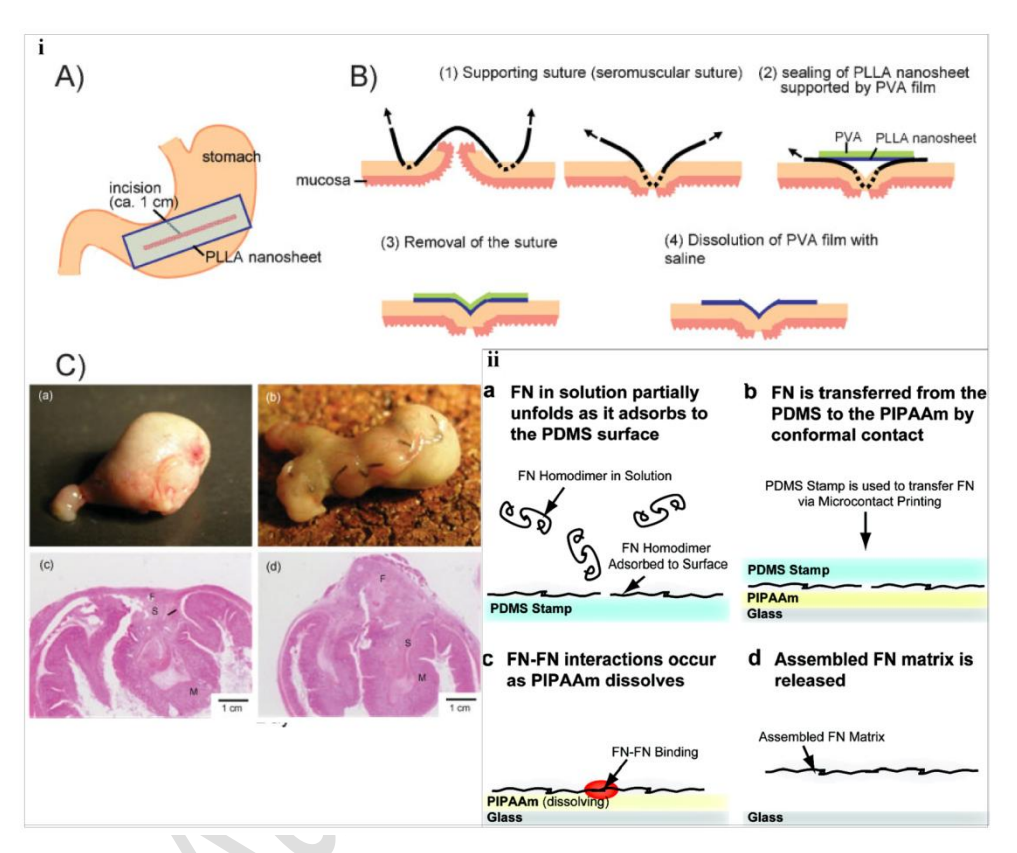


Figure 7. Typical biomedical applications of FUN-membranes

Section i. A) Schematic image of the gastric incision model. B) Schematic images that illustrate sealing of the gastric incision with the PLLA nanomembrane. C) Macroscopic and microscopic observations of the stomach seven days after treatments. Sealing with the PLLA nanomembrane (a, c). Conventional suture/ligation (b, d). Letters F, M, and S show fibroblasts, mucosa, and submucosa, respectively. (Reprinted with permission from (125))

Section ii. A schematic showing the proposed method by which FN homodimers undergo surface-initiated assembly. (a) Soluble FN homodimers in solution adsorb onto PDMS and partially unfold (denature) due to hydrophobic surface interactions. (b) The PDMS surface (typically a stamp for microcontact printing) is placed in conformal contact with a PIPAAm film transferring a portion of the unfolded FN from one surface to the other. (c) The FN on the PIPPAm is hydrated in 37 °C water and then cooled to 35 °C to cause PIPAAm dissolution. (d) As the PIPAAm completely dissolves the assembled FN nanofabric is released as an insoluble, supramolecular structure. (Reprinted with permission from Reference citation 126 (Parker's group). Copyright 2010 American Chemical Society.)

References

- 1. de la Fuente, J. M., and Penades, S. (2006) Biochim Biophys Acta 1760, 636-651
- 2. Jamieson, T., Bakhshi, R., Petrova, D., Pocock, R., Imani, M., and Seifalian, A. M. (2007) Biomaterials 28, 4717-4732
- 3. Beachley, V., and Wen, X. (2010) Progress in Polymer Science 35, 868-892
- 4. Cheng, K., and Sun, S. (2010) Nano Today 5, 183-196
- Liu, T. Y., Hu, S. H., Liu, D. M., Chen, S. Y., and Chen, I. W. (2009) Nano Today 4, 52-65
- Zhang, Y., Lim, C., Ramakrishna, S., and Huang, Z.-M. (2005) Journal of Materials Science: Materials in Medicine 16, 933-946
- 7. Han, D., Pal, S., Liu, Y., and Yan, H. (2010) Nat Nano 5, 712-717
- 8. Zhao, W., Brook, M. A., and Li, Y. F. (2008) Chembiochem 9, 2363-2371
- Vendamme, R., Onoue, S. Y., Nakao, A., and Kunitake, T. (2006) Nat Mater 5, 494-501
- 10. Boisselier, E., and Astruc, D. (2009) Chem Soc Rev 38, 1759-1782
- Podsiadlo, P., Paternel, S., Rouillard, J. M., Zhang, Z. F., Lee, J., Lee, J. W., Gulari, L., and Kotov, N. A. (2005) Langmuir 21, 11915-11921

- 12. Pankhurst, Q. A., Thanh, N. K. T., Jones, S. K., and Dobson, J. (2009) J Phys D Appl Phys 42, -
- 13. Ung, D., Tung, L. D., Caruntu, G., Delaportas, D., Alexandrou, I., Prior, I. A., and Thanh, N. T. K. (2009) Crystengcomm 11, 1309-1316
- 14. Drbohlavova, J., Adam, V., Kizek, R., and Hubalek, J. (2009) Int J Mol Sci 10, 656-673
- Rogach, A. L., Eychmuller, A., Hickey, S. G., and Kershaw, S. V. (2007) Small 3, 536-557
- O'Farrell, N., Houlton, A., and Horrocks, B. R. (2006) Int J Nanomedicine 1, 451-472
- 17. Roca, A. G., Costo, R., Rebolledo, A. F., Veintemillas-Verdaguer, S., Tartaj, P., Gonzalez-Carreno, T., Morales, M. P., and Serna, C. J. (2009) J Phys D Appl Phys 42, -
- Thanh, N. T. K., Puntes, V. F., Tung, L. D., and Fernig, D. G. (2004). in 5th International Conference on Fine Particle Magnetism, London, England
- Baldi, G., Bonacchi, D., Innocenti, C., Lorenzi, G., and Sangregorio, C. (2006). in 6th International Conference on the Scientific and Clinical Applications of Magnetic Carriers, Krems, Austria
- 20. Chen, M., and Nikles, D. E. (2002) J Appl Phys 91, 8477-8479
- Deng, C., Weng, J., Cheng, Q. Y., Zhou, S. B., Lu, X., Wan, J. X., Qu, S. X., Feng, B., and Li, X. H. (2007) Current Applied Physics 7, 679-682
- 22. Hong, Z., Qiu, X., Sun, J., Deng, M., Chen, X., and Jing, X. (2004) Polymer 45, 6699-6706
- Kumar, C. S. S. R., Hormes, J., and Leuschner, C. (2005) Nanofabrication towards biomedical applications: techniques, tools, applications, and impact, Wiley-VCH, Weinheim; Great Britain
- 24. Wang, S. H., Sato, S., and Kimura, K. (2003) Chem Mater 15, 2445-2448
- 25. Turkevich, J., Stevenson, P. C., and Hillier, J. (1951) Discuss Faraday Soc, 55-&

 Lu, L. T., Tung, L. D., Robinson, I., Ung, D., Tan, B., Long, J., Cooper, A. I., Fernig, D. G., and Thanh, N. T. K. (2008) J Mater Chem 18, 2453-2458

- Verma, P. K., Giri, A., Thanh, N. T. K., Tung, L., Mondal, O., Pal, M., and Pal, S. K. (2010) J Mater Chem 20, 3722-3728
- 28. Gnanaprakash, G., Mahadevan, S., Jayakumar, T., Kalyanasundaram, P., Philip, J., and Raj, B. (2007) Mater Chem Phys 103, 168-175
- 29. Stober, W., Fink, A., and Bohn, E. (1968) J Colloid Interf Sci 26, 62-&
- 30. Rogach, A. L. (2000) Mat Sci Eng B-Solid 69, 435-440
- 31. Bao, H. F., Wang, E. K., and Dong, S. J. (2006) Small 2, 476-480
- 32. Daniel, M. C., and Astruc, D. (2004) Chem Rev 104, 293-346
- 33. Gnanaprakash, G., Philip, J., Jayakumar, T., and Raj, B. (2007) J Phys Chem B 111, 7978-7986
- 34. Park, H. S., Dodbiba, G., Cao, L. F., and Fujita, T. (2008) J Phys-Condens Mat 20,
- Sastry, M., Ahmad, A., Khan, M. I., and Kumar, R. (2003) Curr Sci India 85, 162-170
- Ozin, G. A., Arsenault, A. C., and Royal Society of Chemistry (Great Britain).
 (2005) Nanochemistry: a chemical approach to nanomaterials, Royal Society of Chemistry, Cambridge, UK
- 37. Sweeney, S. F., Woehrle, G. H., and Hutchison, J. E. (2006) J Am Chem Soc 128, 3190-3197
- Brust, M., Walker, M., Bethell, D., Schiffrin, D. J., and Whyman, R. (1994) J Chem Soc Chem Comm. 801-802
- 39. Gittins, D. I., and Caruso, F. (2001) Angew Chem Int Edit 40, 3001-3004
- Sun, S. H., Murray, C. B., Weller, D., Folks, L., and Moser, A. (2000) Science 287, 1989-1992
- Murray, C. B., Norris, D. J., and Bawendi, M. G. (1993) J Am Chem Soc 115, 8706-8715

- 42. Gittins, D. I., and Caruso, F. (2001) Angewandte Chemie International Edition 40, 3001-3004
- 43. Cao, H. M., Huang, G. J., Xuan, S. F., Wu, Q. F., Gu, F., and Li, C. Z. (2008) J Alloy Compd 448, 272-276
- 44. Fu, W. Y., Yang, H. B., Hari-Bala, Liu, S. K., Li, M. H., and Zou, G. T. (2006) Mater Lett 60, 1728-1732
- 45. Chakka, V. M., Altuncevahir, B., Jin, Z. Q., Li, Y., and Liu, J. P. (2006) J Appl Phys 99, -
- 46. Becker, A. L., Johnston, A. P. R., and Caruso, F. (2010) Small 6, 1836-1852
- 47. Jiang, C., Markutsya, S., Pikus, Y., and Tsukruk, V. V. (2004) Nat Mater 3, 721-728
- 48. He, Q., Zhang, Z., Xiong, J., Xiong, Y., and Xiao, H. (2008) Optical Materials 31, 380-384
- Kim, J., Kim, H. S., Lee, N., Kim, T., Kim, H., Yu, T., Song, I. C., Moon, W. K., and Hyeon, T. (2008) Angew Chem Int Edit 47, 8438-8441
- Kim, J., Lee, J. E., Lee, J., Yu, J. H., Kim, B. C., An, K., Hwang, Y., Shin, C. H.,
 Park, J. G., Kim, J., and Hyeon, T. (2006) J Am Chem Soc 128, 688-689
- 51. Deng, Y., Qi, D., Deng, C., Zhang, X., and Zhao, D. (2008) J Am Chem Soc 130, 28-+
- Li, Z., Jin, R. C., Mirkin, C. A., and Letsinger, R. L. (2002) Nucleic Acids Res 30, 1558-1562
- 53. An, K., and Hyeon, T. (2009) Nano Today 4, 359-373
- 54. Piao, Y., Kim, J., Na, H. B., Kim, D., Baek, J. S., Ko, M. K., Lee, J. H., Shokouhimehr, M., and Hyeon, T. (2008) Nat Mater 7, 242-247
- Skrabalak, S. E., Chen, J., Au, L., Lu, X., Li, X., and Xia, Y. (2007) Adv Mater Deerfield 19, 3177-3184
- Skrabalak, S. E., Chen, J., Sun, Y., Lu, X., Au, L., Cobley, C. M., and Xia, Y.
 (2008) Acc Chem Res 41, 1587-1595
- 57. Lanone, S., and Boczkowski, J. (2006) Curr Mol Med 6, 651-663

58. Aillon, K. L., Xie, Y. M., El-Gendy, N., Berkland, C. J., and Forrest, M. L. (2009) Adv Drug Deliver Rev 61, 457-466

- 59. Dobrovolskaia, M. A., and Mcneil, S. E. (2007) Nat Nanotechnol 2, 469-478
- 60. Thanh, N. T. K., and Green, L. A. W. (2010) Nano Today 5, 213-230
- 61. Alivisatos, A. P. (1996) Science 271, 933-937
- 62. El-Sayed, M. A. (2001) Accounts Chem Res 34, 257-264
- Chan, W. C. W., Maxwell, D. J., Gao, X. H., Bailey, R. E., Han, M. Y., and Nie, S. M. (2002) Curr Opin Biotech 13, 40-46
- 64. Brus, L. (1986) J Phys Chem-Us 90, 2555-2560
- Galletto, P., Brevet, P. F., Girault, H. H., Antoine, R., and Broyer, M. (1999) J Phys Chem B 103, 8706-8710
- More, R. S., Brack, M. J., Underwood, M. J., and Gershlick, A. H. (1994) Am J Cardiol 73, 1031-1032
- 67. Jain, P., Huang, X., El-Sayed, I., and El-Sayed, M. (2007) Plasmonics 2, 107-118
- Wu, Z. S., Zhang, S. B., Guo, M. M., Chen, C. R., Shen, G. L., and Yu, R. Q. (2007) Anal Chim Acta 584, 122-128
- Otsuka, H., Akiyama, Y., Nagasaki, Y., and Kataoka, K. (2001) J Am Chem Soc 123, 8226-8230
- 70. Han, M. Y., Gao, X. H., Su, J. Z., and Nie, S. (2001) Nat Biotechnol 19, 631-635
- Zhang, C. Y., Yeh, H. C., Kuroki, M. T., and Wang, T. H. (2005) Nat Mater 4, 826-831
- 72. Alivisatos, P. (2004) Nat Biotechnol 22, 47-52
- 73. Chen, Y. J., Chen, S. H., Chien, Y. Y., Chang, Y. W., Liao, H. K., Chang, C. Y., Jan, M. D., Wang, K. T., and Lin, C. C. (2005) Chembiochem 6, 1169-+
- Wakamatsu, H., Yamamoto, K., Nakao, A., and Aoyagi, T. (2006) J Magn Magn Mater 302, 327-333
- 75. Rollings, D. A. E., Tsoi, S., Sit, J. C., and Veinot, J. G. C. (2007) Langmuir 23, 5275-5278

- Zhang, Y., Lim, C. T., Ramakrishna, S., and Huang, Z. M. (2005) J Mater Sci Mater Med 16, 933-946
- 77. Venugopal, J., Low, S., Choon, A. T., and Ramakrishna, S. (2008) Journal of Biomedical Materials Research Part B: Applied Biomaterials 84B, 34-48
- 78. Ma, Z., Kotaki, M., Inai, R., and Ramakrishna, S. (2005) Tissue Engineering 11, 101-109
- 79. Beachley, V., and Wen, X. J. (2010) Progress in Polymer Science 35, 868-892
- 80. Reneker, D. H., and Chun, I. (1996) Nanotechnology 7, 216-223
- 81. Huang, Z. M., Zhang, Y. Z., Kotaki, M., and Ramakrishna, S. (2003) Compos Sci Technol 63, 2223-2253
- 82. Hartgerink, J. D., Beniash, E., and Stupp, S. I. (2001) Science 294, 1684-1688
- 83. Ma, P. X., and Zhang, R. Y. (1999) J Biomed Mater Res 46, 60-72
- 84. Yang, F., Murugan, R., Ramakrishna, S., Wang, X., Ma, Y. X., and Wang, S. (2004) Biomaterials 25, 1891-1900
- 85. Czaja, W. K., Young, D. J., Kawecki, M., and Brown, R. M. (2006) Biomacromolecules 8, 1-12
- 86. Menon, V. P., Lei, J. T., and Martin, C. R. (1996) Chem Mater 8, 2382-2390
- 87. Jeong, H. E., Lee, S. H., Kim, P., and Suh, K. Y. (2006) Nano Letters 6, 1508-1513
- 88. Beachley, V., and Wen, X. (2010) Prog Polym Sci 35, 868-892
- 89. Fertala, A., Han, W. B., and Ko, F. K. (2001) J Biomed Mater Res 57, 48-58
- Li, W. J., Laurencin, C. T., Caterson, E. J., Tuan, R. S., and Ko, F. K. (2002) J Biomed Mater Res 60, 613-621
- Li, W. J., Danielson, K. G., Alexander, P. G., and Tuan, R. S. (2003) J Biomed Mater Res A 67, 1105-1114
- 92. Yoshimoto, H., Shin, Y. M., Terai, H., and Vacanti, J. P. (2003) Biomaterials 24, 2077-2082
- 93. Huang, L., McMillan, R. A., Apkarian, R. P., Pourdeyhimi, B., Conticello, V. P., and Chaikof, E. L. (2000) Macromolecules 33, 2989-2997

 Nagapudi, K., Brinkman, W. T., Leisen, J. E., Huang, L., McMillan, R. A., Apkarian, R. P., Conticello, V. P., and Chaikof, E. L. (2002) Macromolecules 35, 1730-1737

- 95. Mo, X. M., Xu, C. Y., Kotaki, M., and Ramakrishna, S. (2004) Biomaterials 25, 1883-1890
- 96. Hardy, C. J., Zhao, L., Zong, X., Saranathan, M., and Yucel, E. K. (2003) J Magn Reson Imaging 17, 170-176
- Silva, G. A., Czeisler, C., Niece, K. L., Beniash, E., Harrington, D. A., Kessler, J. A., and Stupp, S. I. (2004) Science 303, 1352-1355
- 98. Curtis, A., and Wilkinson, C. (2001) Trends Biotechnol 19, 97-101
- Craighead, H. G., James, C. D., and Turner, A. M. P. (2001) Curr Opin Solid St M 5, 177-184
- 100. Ignatious, F. E., PA, US), Baldoni, John M. (Glenmoore, PA, US). (2003) Electrospun pharmaceutical compositions. United States
- 101. Zong, X. H., Li, S., Chen, E., Garlick, B., Kim, K. S., Fang, D. F., Chiu, J., Zimmerman, T., Brathwaite, C., Hsiao, B. S., and Chu, B. (2004) Ann Surg 240, 910-915
- 102. Wang, X., Kim, Y.-G., Drew, C., Ku, B.-C., Kumar, J., and Samuelson, L. A. (2004) Nano Letters 4, 331-334
- 103. Wang, X., Drew, C., Lee, S.-H., Senecal, K. J., Kumar, J., and Samuelson, L. A. (2002) Nano Letters 2, 1273-1275
- 104. Cheng, W. L., Campolongo, M. J., Tan, S. J., and Luo, D. (2009) Nano Today 4, 482-493
- 105. Han, J., and Craighead, H. G. (2000) Science 288, 1026-1029
- 106. Striemer, C. C., Gaborski, T. R., McGrath, J. L., and Fauchet, P. M. (2007) Nature 445, 749-753
- 107. Toh, C. S., Kayes, B. M., Nemanick, E. J., and Lewis, N. S. (2004) Nano Letters 4, 767-770

- 108. Cheng, W., Campolongo, M. J., Tan, S. J., and Luo, D. (2009) Nano Today 4, 482-493
- 109. Lin, Y., Skaff, H., Emrick, T., Dinsmore, A. D., and Russell, T. P. (2003) Science 299, 226-229
- 110. Lin, Y., Boker, A., Skaff, H., Cookson, D., Dinsmore, A. D., Emrick, T., and Russell, T. P. (2005) Langmuir 21, 191-194
- 111. Boker, A., He, J., Emrick, T., and Russell, T. P. (2007) Soft Matter 3, 1231-1248
- 112. Yang, H., Coombs, N., Sokolov, I., and Ozin, G. A. (1996) Nature 381, 589-592
- 113. Goedel, W. A., and Heger, R. (1998) Langmuir 14, 3470-3474
- 114. Mallwitz, F., and Goedel, W. A. (2001) Angewandte Chemie International Edition 40, 2645-2647
- 115. Xu, H., and Goedel, W. A. (2002) Langmuir 18, 2363-2367
- 116. Bigioni, T. P., Lin, X. M., Nguyen, T. T., Corwin, E. I., Witten, T. A., and Jaeger, H. M. (2006) Nat Mater 5, 265-270
- 117. Lin, X. M., Jaeger, H. M., Sorensen, C. M., and Klabunde, K. J. (2001) J Phys Chem B 105, 3353-3357
- 118. Cheng, W. L., Park, N. Y., Walter, M. T., Hartman, M. R., and Luo, D. (2008) Nat Nanotechnol 3, 682-690
- Cheng, W. L., Campolongo, M. J., Cha, J. J., Tan, S. J., Umbach, C. C., Muller, D.
 A., and Luo, D. (2009) Nat Mater 8, 519-525
- 120. Vlassak, J. J., and Nix, W. D. (1992) J Mater Res 7, 3242-3249
- 121. Markutsya, S., Jiang, C. Y., Pikus, Y., and Tsukruk, V. V. (2005) Adv Funct Mater 15, 771-780
- 122. Watanabe, H., Vendamme, R., and Kunitake, T. (2007) B Chem Soc Jpn 80, 433-440
- 123. Stafford, C. M., Harrison, C., Beers, K. L., Karim, A., Amis, E. J., Vanlandingham, M. R., Kim, H. C., Volksen, W., Miller, R. D., and Simonyi, E. E. (2004) Nat Mater 3, 545-550

124. VanLandingham, M. R., Villarrubia, J. S., Guthrie, W. F., and Meyers, G. F. (2001) Macromol Symp 167, 15-43

- 125. Okamura, Y., Kabata, K., Kinoshita, M., Saitoh, D., and Takeoka, S. (2009) Advanced Materials 21, 4388-4392
- 126. Feinberg, A. W., and Parker, K. K. (2010) Nano Letters 10, 2184-2191